Results in Engineering 25 (2025) 103889

Contents lists available at ScienceDirect

Results in Engineering

journal homepage: www.sciencedirect.com/journal/results-in-engineering

Research paper

Crashworthiness characteristic of aluminum/composite hybrid tubes under axial compression

Willy Artha Wirawan [a,*], Ayan Sabitah [b], Gunawan Sakti [a], Bambang Bagus Harianto [a], Moch. Agus Choiron [c], R.A. Ilyas [d], S.M. Sapuan [e], Joewono Prasetijo [f]

[a] Department of Aircraft Engineering, Politeknik Penerbangan Surabaya, Jemur Andayani I No 73 Wonocolo, Surabaya, Indonesia
[b] Politeknik Negeri Banjarmasin, Jl. Brig Jend. Hasan Basri, Kalimantan, 70124 Indonesia
[c] Mechanical Engineering Department, Brawijaya University, Mayjen Haryono Street 165 Malang, 65145, Indonesia
[d] Department of Chemical Engineering, Faculty of Chemical and Energy Engineering, Universiti Teknologi Malaysia, 81310, Johor Bahru, Johor, Malaysia
[e] Advanced Engineering Materials and Composite Research Centre (AEMC), Department of Mechanical and Manufacturing Engineering, Universiti Putra Malaysia, 43400 UPM Serdang, Selangor, Malaysia
[f] Universiti Tun Hussein Onn Malaysia, 86400 Parit Raja, Batu Pahat, Johor Darul Ta'zim, Malaysia

ARTICLE INFO

Keywords:
Crashworthiness
Hybrid tubes
Axial compression
Energy absorption
Natural fiber reinforcement
Quasi-static test
Progressive crushing behavior
Structural energy absorption efficiency

ABSTRACT

This study investigates the crashworthiness performance and energy absorption characteristics of circular aluminum-composite hybrid tubes reinforced with layers of waru bark fiber. Four tube configurations were fabricated: Aluminum Circular Tube (ACT), Composite Circular Tube (CCT), Hybrid Inner Circular Tube (HICT), and Hybrid Outer Circular Tube (HOCT). These tubes were subjected to quasi-static axial compression loading tests. The reinforcement layers, oriented at 0°–90°, were bonded using epoxy resin. The experimental results revealed that the addition of reinforcement layers introduced new progressive crushing behaviors, such as internal curling and corkscrew patterns, which effectively mitigated buckling failure. The hybrid designs significantly enhanced energy absorption, with HOCT and HICT achieving improvements of 49.18% and 43.78%, respectively, compared to the unreinforced ACT. Among the configurations, HOCT demonstrated the highest crashworthiness, with a peak crushing force (IPFC) of 42.36 kN, a mean force (MF) of 24.66 kN, and a crush force efficiency (CFE) of 0.49%. However, the specific energy absorption (SEA) decreased as tube diameter and reinforcement density increased. These results offer valuable insights into the optimization of reinforced composite tube designs, highlighting their potential for advanced crashworthiness and energy absorption applications.

1. Introduction

The advancement of security system technology in transportation and the growing demand for community mobility are becoming increasingly significant. According to data from the Indonesian Statistical Agency, the number of traffic accidents recorded in 2017–2018 reached 116.411 cases, resulting in 25.671 fatalities. These statistics highlight the urgent need to integrate safety technologies into transportation equipment manufacturing to mitigate the impact of accidents. Among passive safety technologies, crashworthiness plays a pivotal role. A crashworthy system functions as an energy absorber, reducing collision severity through controlled deformation mechanisms. [1]. Crashworthiness is typically achieved using thin-walled circular tube structures designed to undergo permanent deformation upon impact. These circular tubes are widely utilized due to their superior specific energy absorption capacity and ease of fabrication [2,3].

In the typical behavior of energy-absorbing tubes made from metallic materials such as mild steel or aluminum, energy is generally absorbed through plastic deformation mechanisms [4–6]. Studies on thin-walled energy-absorbing tubes using metallic materials have demonstrated that their performance can be enhanced by incorporating metal fillers, polymer foams, or reinforcement layers made of composite materials, effectively reducing axisymmetric plastic buckling modes [7,8]. These designs have been further developed to achieve tubes with higher energy absorption capacities [9].

Further research on thin-walled tubes has explored the incorporation

* Corresponding author.
E-mail address: willyartha@poltekbangsby.ac.id (W.A. Wirawan).

https://doi.org/10.1016/j.rineng.2024.103889
Received 16 October 2024; Received in revised form 23 December 2024; Accepted 31 December 2024
Available online 1 January 2025

of new materials, such as composite materials derived from natural fibers [10]. The addition of these composite materials to thin-walled aluminum tubes is shown to enhance their energy absorption capacity significantly [11,12]. The collapse behavior of composite fiber materials in energy-absorbing tubes demonstrates progressive crushing and fracture patterns [13,14]. Natural fiber-reinforced composites in hybrid tubes offer several advantages, including high impact resistance, a high strength-to-weight ratio, ease of installation, malleability, and lightweight properties [15,16]. Incorporating natural fibers into hybrid composite structures aims to enhance performance and mitigate the limitations of individual materials in energy-absorbing tubes, making it a promising area for further exploration [17].

Recently, there has been growing interest among researchers and environmentalists in products made from natural fiber composites. The primary motivations for developing such products are environmental sustainability and the shift toward more eco-friendly energy solutions [18]. Research on natural fiber-reinforced composites is highly diverse, encompassing various types of fibers, matrices, and manufacturing methods to produce materials with superior mechanical properties while maintaining environmental friendliness. Numerous natural fibers have been explored, including sisal, jute, kenaf, and waru fibers [19]. The abundant availability of lignocellulosic fibers in tropical countries presents significant opportunities for their development in various applications, such as hybrid crashworthiness materials.

Studies on hybrid energy-absorbing tubes based on natural fiber composites are relatively limited. The initial exploration and development of natural fiber-based hybrid energy-absorbing tubes utilized kenaf-epoxy fiber. The results indicated that a kenaf fiber hybrid tube with a winding orientation angle of 70° could enhance energy absorption by 56%. Additionally, it exhibited a more favorable progressive crushing failure mode compared to buckling failure [20,21]. Furthermore, the study examined the effect of winding orientation on the performance of hybrid and non-hybrid kenaf composite tubes. The findings demonstrated that the hybrid effect improved progressive crushing behavior by incorporating a combination of local buckling, delamination fractures, and brittle fractures as part of the crushing mechanism [22]. Regarding the aspect of winding orientation, results showed that higher winding orientations in hybrid composite tubes significantly enhanced crush load efficiency, specific energy absorption, and overall energy absorption capability compared to glass fiber-reinforced polymer (GFRP) composite tubes [23–26]. The development of crashworthiness designs has advanced considerably, with recent studies on hybrid effects revealing diverse crashworthiness behaviors and optimal configurations that improve energy absorption. Hybrid composites in energy absorption tube studies, such as metal/natural fiber-reinforced polymers, have been identified as effective in increasing crashworthiness and overall energy absorption capacity [27,21,28].

The combination of aluminum with carbon fiber-reinforced polymer (CFRP) and glass fiber-reinforced polymer (GFRP) significantly enhances the specific energy absorption (SEA) capacity compared to single-material tubes. For example, aluminum-CFRP hybrid tubes achieve an SEA of 2.41 J/g, representing a 58% increase compared to the combined contributions of individual aluminum and CFRP components. Similarly, aluminum-GFRP hybrid tubes demonstrate a 47% improvement in SEA. Moreover, a symmetric stacking sequence, such as [CF-P4-AL-T1]s, has been shown to achieve the highest SEA of 3.43 J/g in aluminum-CFRP hybrid systems [29].

Compared to synthetic fiber-based hybrid systems, recent studies have also investigated the use of natural fibers, such as ramie, in combination with glass fibers. Although natural fibers offer benefits such as a 22% weight reduction and lower production costs, their mechanical performance and crashworthiness remain inferior to those of synthetic fibers [15]. Meanwhile, tri-hybrid aluminum-CFRP-GFRP tubes demonstrate an SEA improvement of 4.90% compared to aluminum-GFRP configurations. This enhancement is attributed to the GFRP layers on the outer surface, which provide additional flexibility, while the CFRP layers contribute to increased structural stiffness [25]. Further research highlights the importance of optimizing parameters such as stacking sequence, hybrid ratio, and layer thickness of aluminum and composite materials to achieve superior energy absorption performance.

The growing interest in hybrid composite energy-absorbing tubes has prompted research into using natural fibers as reinforcements to improve impact resistance and energy absorption. Hybridization with natural composites offers innovative prospects for high-performance systems. This study investigates using Hibiscus tiliaceus fibers as reinforcements in hybrid composites, incorporating layers on aluminum tubes' inner and outer surfaces. The findings highlight the potential of such designs to enhance crashworthiness and energy absorption efficiency, advancing natural fiber-reinforced hybrid tubes as viable solutions for energy absorption systems.

2. Materials and methods

2.1. Materials

In this study, Al 6063-T5 is utilized as the metallic material. Based on the results of material testing (Fig. 1), the specific properties of the material are as follows:the specific properties of the material were determined as follows : density ρ =2700 kg/m^3, Young's modulus E = 66 GPa, Poisson's ratio ν =0.33, Yield stress σs = 72.68 MPa, ultimate stress σb = 99.62 MPa and Tangent Modulus H = 278.84 MPa. The composite material consists of a natural fiber composite made from waru bark fiber and epoxy resin, with its material properties detailed in Table 1.

2.2. Geometric and tube design

The proposed hybrid design concept utilizing natural fibers as reinforcement holds significant potential for the development of high-performance, environmentally friendly energy-absorbing tubes. Moreover, the simplicity of manufacturing these tubes, due to their conventional straight-tube geometry Fig. 2 enhances their practical feasibility. Incorporating Composite Circular Tubes (CCT) on both the outer and inner surfaces effectively mitigates buckling, facilitating controlled folding mechanisms that significantly increase the maximum force (F max) achieved during compression.

This study examines the energy absorption performance of a hybrid crashworthiness Aluminum Circular Tube (ACT) and Composite Circular Tube (CCT) system across four specimen models.

Model I Composite Circle Tube (CCT): composite tube is constructed using natural waru bark fiber as reinforcement and an epoxy matrix.
Model II Aluminium Circle Tube (ACT): metallic tube fabricated from Al-6063-T5 aluminum alloy with a circular cross-section
Model III Hybrid Inner Circle Tube (HICT): aluminum metal tube lined with a Composite Circular Tube (CCT) layer on its inner surface.
Model IV Hybrid Outer Circle Tube (HOCT): aluminum metal tube encased in a Composite Circular Tube (CCT) layer on its outer surface.

The external dimensional parameters of the aluminum tubes were designed with a fixed inertial cross-section, and the following dimensions were constructed to ensure manufacturing accuracy of the specimens. The aluminum tubes have a length (l) = = 150 mm, external diameter (d) = 65 mm, thickness (t) = 1.5 mm, and tube end chamfer angle (φ) = 45°. Additionally, composite tubes with a fiber angle orientation of 0/90° and three layers were added to the outer and inner sides of the aluminum tubes. The details of the crashworthiness specimen dimensions for each specimen made in this study can be seen in Table 2.

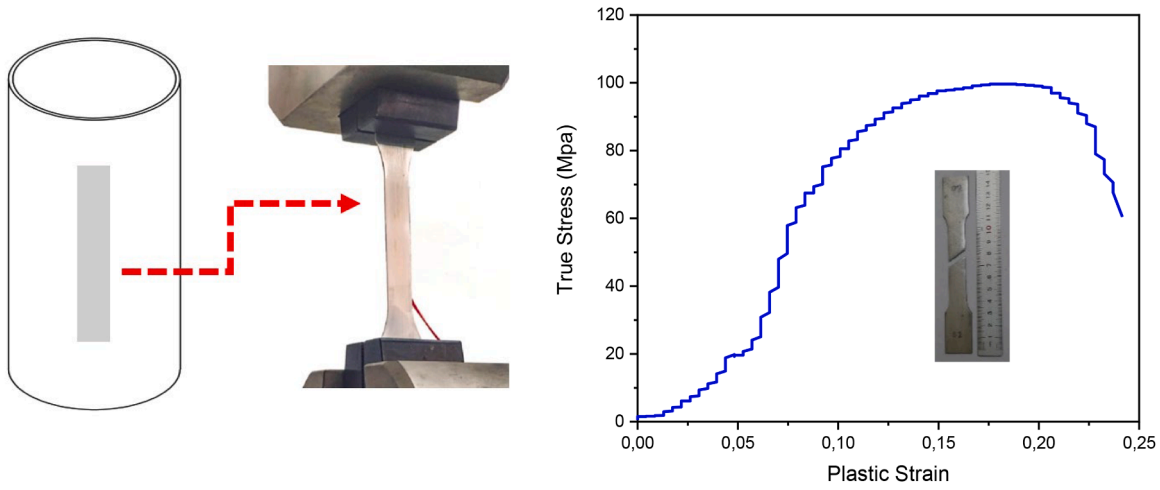

Fig. 1. True strain–stress curves of Al 6063-T5.

Table 1
Material properties of natural fiber composite [19,30].

Properties	Value
Young's Modulus X direction (MPa)	401.36
Young's Modulus Y direction (MPa)	401.36
Young's Modulus Z direction (MPa)	65.23
Poisson's Ratio XY	0.04
Poisson's Ratio YZ	0.3

2.3. Hybrid specimen crashworthiness

The hybrid crashworthiness manufacturing process was carried out by continuously spinning waru fibers on the aluminum surface by forming a 2-2 basket weave pattern, ± 10 mm fiber diameter, and 0/90 fiber orientation angle. Waru fibers were spun on the outer side for HOCT specimens, while inner fibers were spun for HICT specimens. The fibers were then enclosed in a circular mold and processed using the vacuum infusion method, as illustrated in Fig. 3. The vacuum infusion process was conducted with a VALUE VE280N vacuum machine, featuring an ultimate vacuum of 15 microns and a free air displacement flow rate of 9.0 FCM.

After completing the molding process using the vacuum infusion method, the specimens were cleaned and dried at room temperature ± 23℃ for six days. Subsequently, the specimens were inspected and measured for length (l), diameter (d), thickness (t), and mass (m). The preparation and selection of specimens were conducted rigorously to ensure sample homogeneity prior to quasi-static testing. Each quasi-static crashworthiness test specimen used in this study is shown in Fig. 4.

2.4. Quasi-static - axial crushing test experiments

In this study, quasi-static crushing experiments were performed using a 300 kN SHIMADZU Universal Testing Machine (UTM) from Japan. The quasi-static test was conducted by positioning the specimen on the fixed support of the testing machine, after which the impactor, functioning as a rigid body, compressed the tube at a constant speed of 2 mm/s, as illustrated in Fig. 5. During the compression, the displacement distance was controlled at 75% of the tube height, approximately 100 mm. The testing machine recorded the force response and displacement data throughout the experiment. Mechanical fracture behavior was documented using a Canon PowerShot SX430 IS digital camera [31,25].

2.5. Crashworthiness performance

Common criteria for evaluating crashworthiness include Specific Energy Absorption (SEA), Mean Force (MF), Initial Peak Force (IPFC), Crush Force Efficiency (CFE), and Energy absorption (EA) [31,32]. EA represents the total energy absorbed during impact, which is determined by calculating the area under the load-displacement curve. The energy absorption is mathematically expressed using the following integral equation.

$$EA = \int_0^d f(\delta)d\delta \tag{1}$$

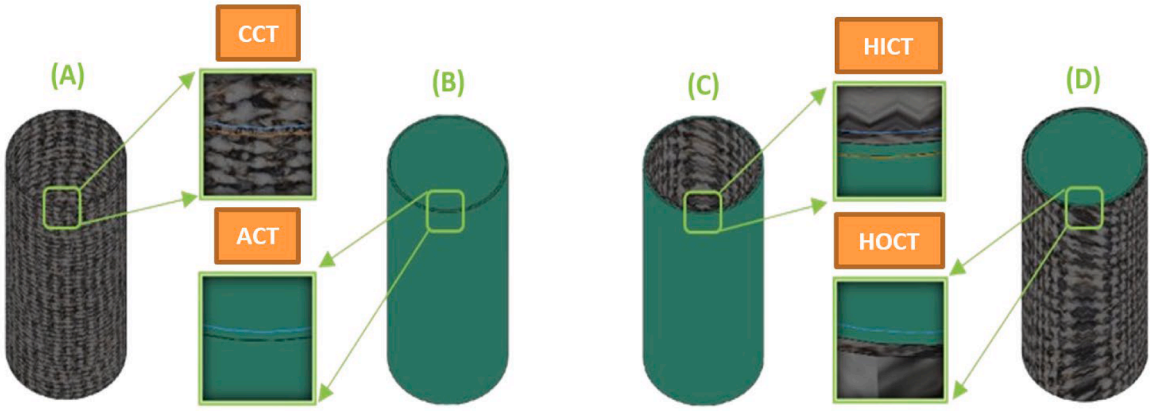

Fig. 2. Tube models (a) Composite Circle Tube (CCT) (b) Aluminium Circle Tube (ACT) (c) Hybrid Inner Circle Tube (HICT) (d) Hybrid Outer Circle Tube (HOCT).

Table 2
Dimensions of the primary specimens of the crashworthiness outer section.

Specimen crashworthiness	Tube number	d (mm)	t (mm)	l (mm)	m (g)
Composite Circle Tube (CCT)	NCT-1	65.1	1.50	150.1	40.1 (± 0.5)
	NCT-2	65.0	1.52	150.0	39.9 (± 0.5)
	NCT-3	65.2	1.52	150.3	40.9 (± 0.5)
Aluminium Circle Tube (ACT)	CT-1	65.0	1.50	150.0	106.1 (± 0.1)
	CT-2	65.0	1.50	150.0	106.1 (± 0.1)
	CT-3	65.0	1.50	149.8	105.9 (± 0.1)
Hybrid Inner Circle Tube (HICT)	HICT-1	65.0	3.30	150.2	146.7 (± 0.4)
	HICT-2	65.0	3.10	149.9	145.9 (± 0.4)
	HICT-3	65.0	3.10	150,0	146.3 (± 0.4)
Hybrid Outer Circle Tube (HOCT)	HOCT-1	68,0	3.10	149.8	146.9 (± 0.3)
	HOCT-2	68.1	3.20	150.0	147.4 (± 0.3)
	HOCT-3	68.2	3.10	150.1	148.8 (± 0.3)

$F(\delta)$ is the crushing force and crushing distance

MF represents the average load exerted on the crusher as the energy absorber transitions to a stable form. It is defined mathematically by the following equation.

$$MF = \frac{1}{d}\int_0^d f(\delta)d\delta \tag{2}$$

Crush Force Efficiency (CFE) is defined as the average ratio of the crushing force, calculated by dividing the mean force (MF) by the initial peak force (IPFC).

$$\text{CFE} = \frac{MF}{IPFC} x\ 100 \tag{3}$$

Specific Energy Absorption (SEA) is a criterion used to quantify the energy absorbed (EA) per unit mass, serving as a critical indicator of a structure's energy absorption capability. SEA is determined using the following mathematical equation.

$$\text{SEA} = \frac{EA}{m} \tag{4}$$

3. Results and discussion

3.1. Load-displacement response

Fig. 6 illustrates the graph depicting the relationship between load and displacement. Generally, it is evident that during the initial phase of loading, a significant force is required to compress the tube, resulting in the generation of the initial peak force. This phase marks the beginning of the energy absorption process, where the impactor's push causes progressive folding, leading to an increase in the reaction force for each crashworthiness model.

In Fig. 6. it can be observed that folding occurs sequentially across the crashworthiness designs, beginning with the ACT design, followed by the HICT design, and finally the HOCT design. The crashworthiness ACT design exhibits a peak reaction force of 42,369.39 N, initiating folding and forming the first ring at 4.61 mm. In the ACT design, six folding events are observed, with the second and sixth foldings showing a consistent reaction force value of 25,037.08 N. The second folding occurs at 21.96 mm, the third at 39.52 mm, the fourth at 55.59 mm, the fifth at 72.24 mm, and the final folding at 88.26 mm.

The crashworthiness Hybrid Inner Circle Tube (HICT) design exhibits

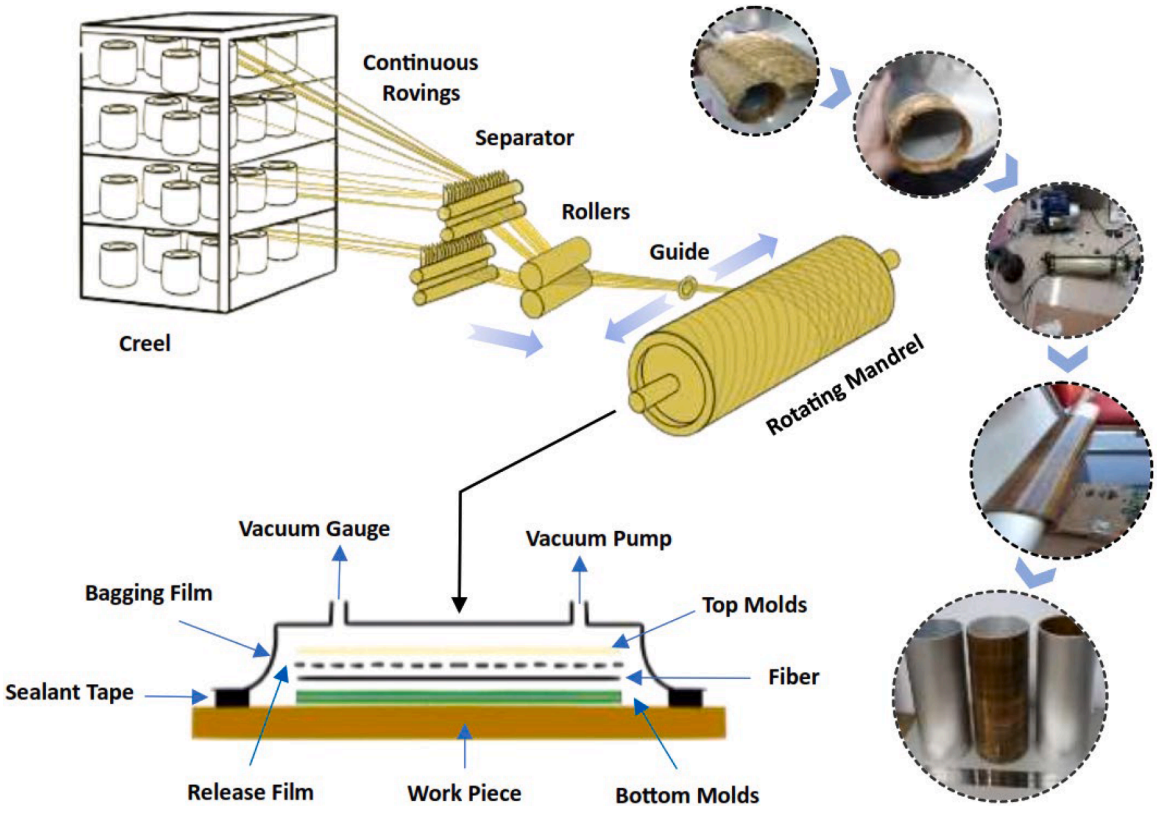

Fig. 3. The hybrid crashworthiness design manufacturing process is made from ACT/CCT using filament winding and vacuum infusion methods.

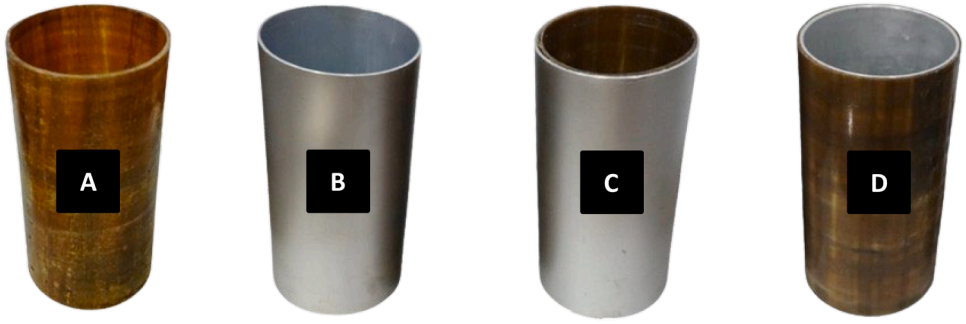

Fig. 4. Crashworthiness specimens (a) CCT (b) ACT (c) HICT (d) HOCT.

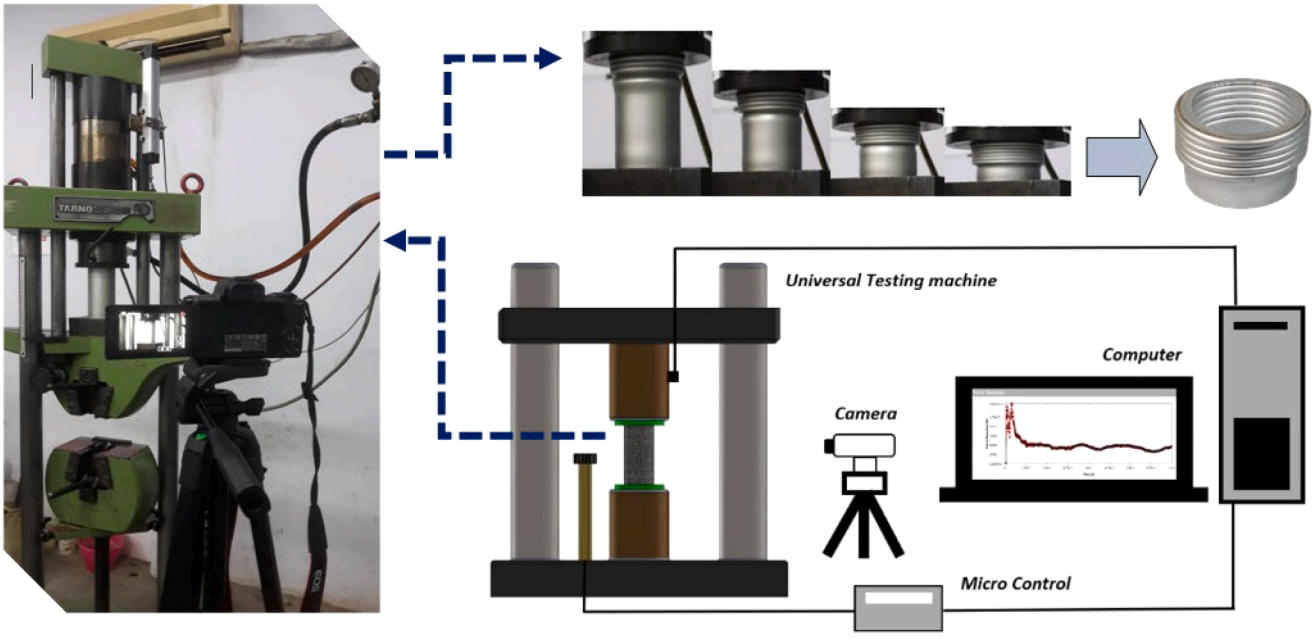

Fig. 5. Quasi-static crashworthiness testing scheme.

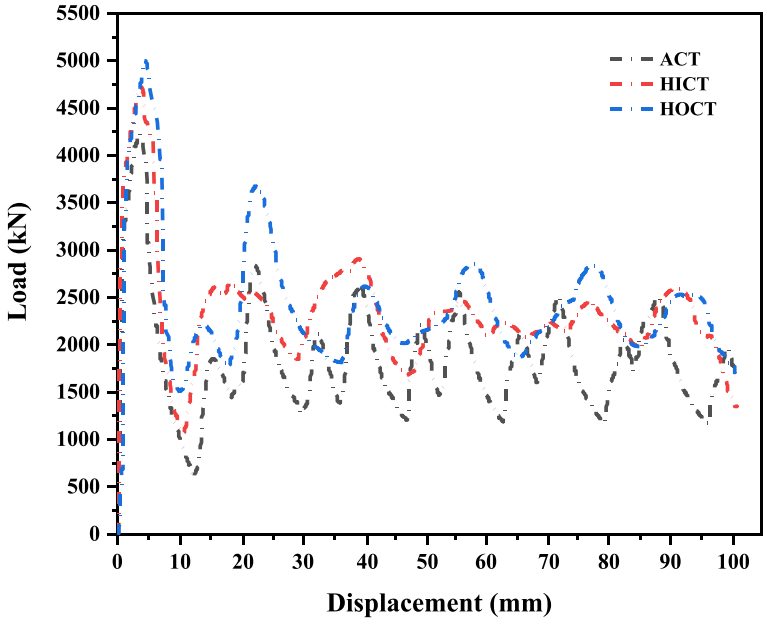

Fig. 6. Load-displacement response of hybrid crashworthiness.

a peak reaction force of 47,217.49 N. The initial phase of displacement begins with folding caused by the debonding of the aluminum and composite materials under the impactor load, forming a fold at 3.74 mm. The crashworthiness HICT design shows uneven and irregular reaction peak values compared to the ACT and HOCT designs. This irregularity may result from the composite material on the inner surface undergoing progressive collapse [11]. The impact energy is partially dissipated before the tube is fully destroyed. The combined interaction between the aluminum and the failed composite material plays a significant role in this behavior.

The crashworthiness Hybrid Outer Circle Tube (HOCT) design exhibits a peak reaction force of 49,983.91 N. The initial phase of displacement begins with the aluminum and composite materials forming similar folding patterns, with the first folding occurring at 4.61 mm. Subsequent folding occurs at 22.4 mm, 39.52 mm, 58.19 mm, 77.73 mm, and 92.44 mm. Analysis of the load-displacement curve reveals that the HOCT and ACT crashworthiness designs exhibit similar reaction peak characteristics. However, the HOCT design demonstrates a more effective crushing distance and strain rate effect [33]. This indicates that the addition of composite materials in the HOCT design enhances rigidity and achieves more complete plastic deformation [22].

3.2. Initial peak crushing force (IPFC)

Thin-walled tubes generally exhibit an initial peak crushing force during the early stage of a collision. This peak force, referred to as the initial or highest peak force, occurs at the onset of the crushing process. Under actual conditions, when absorbing crash energy, the crashworthiness design often experiences an excessively high initial peak force compared to the subsequent folding stages. This may result in a buckling phenomenon and a reduction in energy absorption efficiency [34]. The initial Peak Crushing Force for each crashworthiness design is shown in Fig. 7.

In Fig. 7, it is evident that adding layers of reinforcement using waru fiber composite material contributes to an increase in peak force and pre-crushing values. Experimental results indicate that during the initial stage of the impactor striking the crashworthiness structure, the peak force of each hybrid crashworthiness design increased without any observable buckling phenomenon. This serves as evidence that the axial loading force (Peak Force) can effectively resist initial deformation in a stable manner. Following this, a sharp fluctuation in force (secondary force) occurs, followed by an increase in force (first fold). The Initial Peak Crushing Force (IPFC) values for the Crashworthiness Circle Tube, Hybrid Inner Circle Tube (HICT), and Hybrid Outer Circle Tube (HOCT) designs are 42.36 kN, 47.21 kN, and 49.98 kN, respectively. The increased IPFC in hybrid crashworthiness designs can be attributed to the enhanced force response provided by the waru fiber composite material. The IPFC is also influenced by the presence of materials that significantly enhance the stiffness of the composite tube at displacement values between 2 mm and 4 mm [35]. Due to the alignment of the fibers, the hybrid tubes exhibit greater load-bearing capacity before collapsing, benefiting from the superior impact resistance and high fracture energy of the fibers. This phenomenon is also observed in crashworthiness designs utilizing CFRP tubes, where the structure responds with higher resistance at the IPFC during impact loading [36]. The IPFC response of the HICT design is slightly lower than that of the HOCT design, likely due to the composite frame reinforcement being located on the inner wall in HICT. In HICT, the deformation of the composite skeleton on the unstable inner wall causes twisting and cracking into large fragments at the onset of impact. The twisted composite skeleton applies lateral compression to the inner tube wall, acting as a blade trigger and reducing the initial peak force. This behavior is further evidenced by the uneven and less stable secondary force and first fold [13].

3.3. Crashworthiness characteristics

The performance characterization of hybrid tube structures, encompassing key parameters such as Energy Absorption (EA), Mean Force (MF), Specific Energy Absorption (SEA), and Crush Force Efficiency (CFE), is comprehensively depicted in Fig. 8. This analysis offers a detailed evaluation of the structural efficiency and energy absorption capacity, which are essential for assessing the effectiveness and reliability of the hybrid tube design under specific loading conditions.

The highest energy absorption value is observed in the HOCT crashworthiness design, with an absorption value of 2.76 kJ, while the lowest energy absorption value is recorded in the ACT crashworthiness design, at 1.85 kJ. The superior energy absorption in the HOCT design is attributed to the addition of a reinforcement layer on the outer tube wall. Since energy absorption is directly proportional to the applied load, a higher load results in greater energy absorption. The addition of a reinforcement layer to the composite significantly influences crashworthiness parameters [37,38]. As highlighted in Haiyang Yang's research, the energy absorption in CFRP/GFRP tubes generally increases with the number of GFRP layers due to the enhanced force response of the material [13]. The improved energy absorption in the HOCT crashworthiness design is also influenced by the increased thickness of the deformed outer crashworthiness wall's cross-sectional area, which enhances the moment of inertia. According to Euler's equation, the moment of inertia is directly proportional to the critical load, meaning that a higher critical load leads to greater energy absorption.

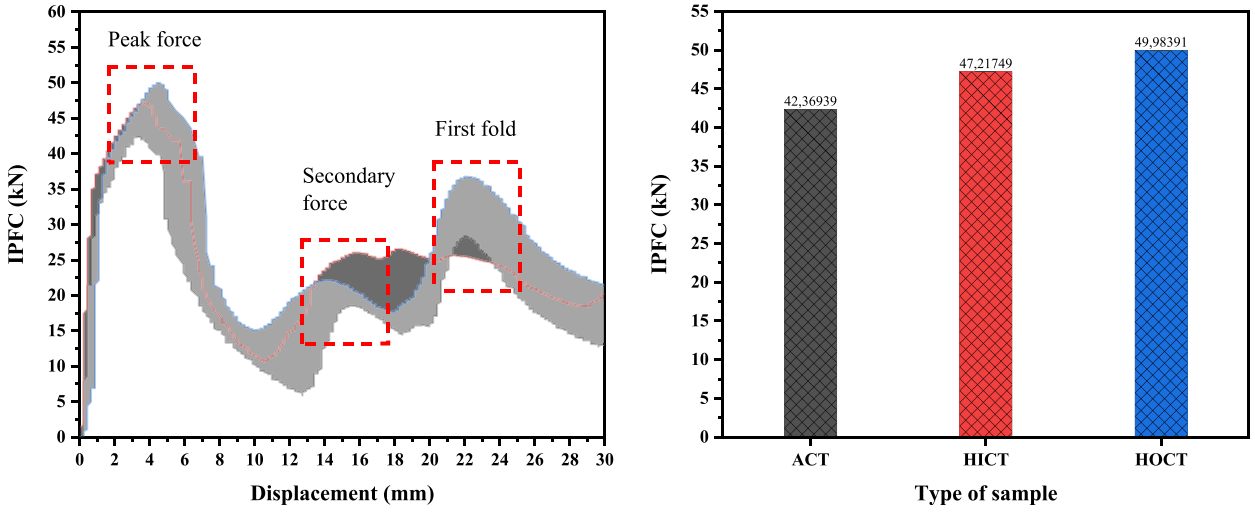

Fig. 7. Initial Peak Crushing Force (IPFC).

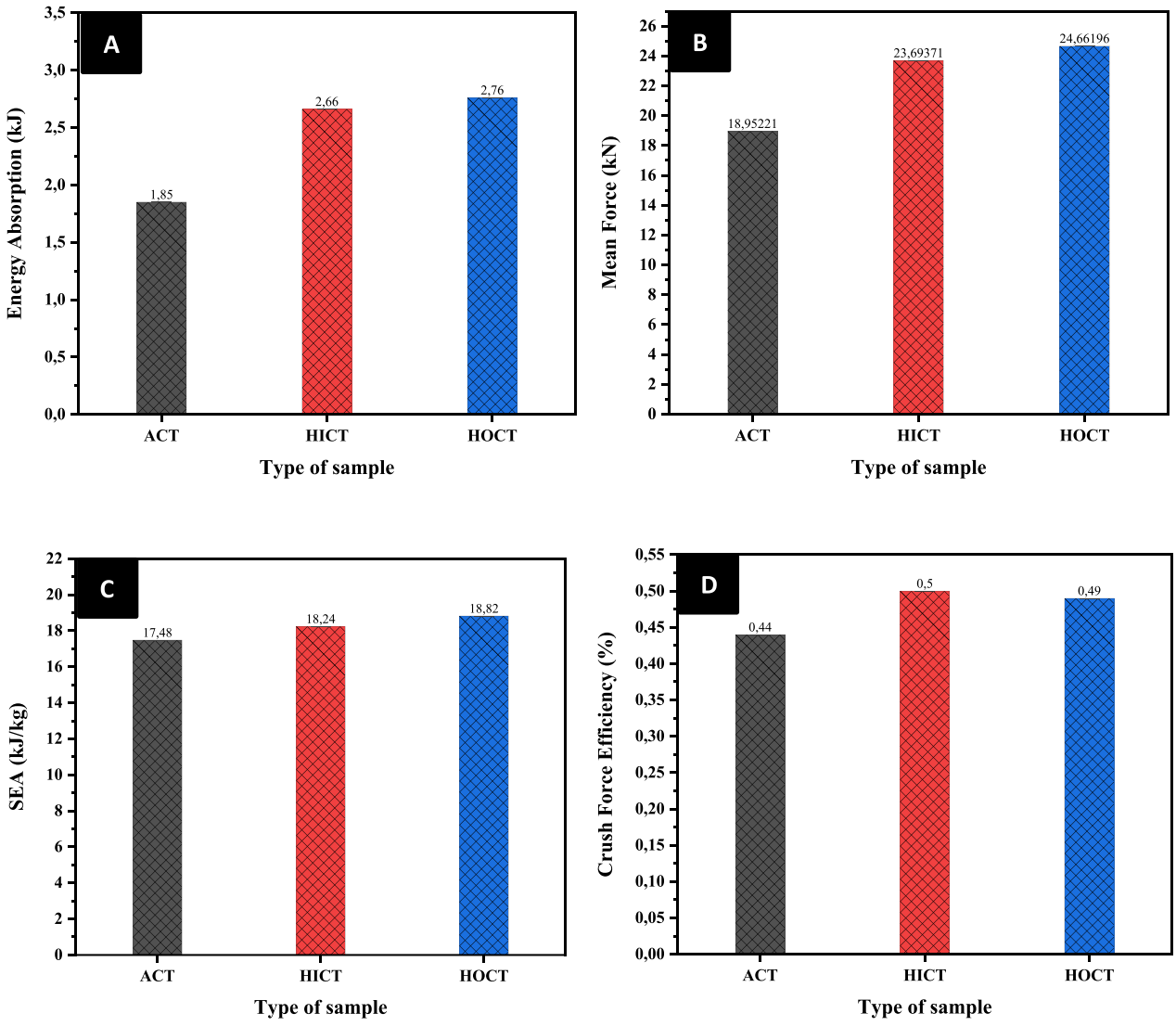

Fig. 8. (a) EA (b) MF (c) SEA (d) CFE.

From the load-displacement graph, the MF value was calculated as the average peak force of each crashworthiness design. The mean force region represents the amplitude of the mean oscillation force, indicating the force required to initiate and propagate new folds. The results demonstrate that the MF value is directly proportional to the energy absorption (EA) of each design. The MF value varies depending on the crushing test parameters, with the ACT design showing an MF of 18.95 kN, the HICT design 23.69 kN, and the HOCT design achieving the highest MF of 24.66 kN. The load-displacement curves further indicate that the average force ratio increases by 25% for the HICT design and 30% for the HOCT design. A corresponding trend is observed in energy absorption. The addition of composite material on the inner side of the HICT design leads to a collapse mechanism, resulting in uneven peak force values and lower MF compared to the HOCT design. Consequently, adding a reinforcement layer to the outer side, as in the HOCT design, is recommended to provide a more stable folding sequence with reduced peak and average forces, offering improved crashworthiness performance. [39].

The comparison of energy absorption capabilities for different materials and structures, represented in the load-displacement curve, is quantified as specific energy absorption (SEA). The SEA values for each crashworthiness design are presented in Fig. 7b. The crashworthiness ACT design exhibits an SEA value of 17.48 kJ/kg, the HICT design shows an increased SEA value of 18.24 kJ/kg, and the HOCT design achieves the highest SEA value of 18.82 kJ/kg. The increased SEA in the HICT and HOCT designs is attributed to the addition of reinforcement layers using waru fiber composites, resulting in higher performance compared to the ACT design, which lacks composite reinforcement. The energy absorption characteristics of hybrid tubes with pure aluminum and composite materials reveal that lightweight hybrid tubes exhibit superior specific energy absorption capabilities [9,40]. Similarly, a crashworthiness study by Reuter and Troster on circular-section hybrid aluminum/CFRP tubes demonstrated that the specific energy absorption of the hybrid mechanism was higher than that of pure aluminum structures [41].

Another critical metric for evaluating crush performance is Crush Force Efficiency (CFE), which measures the crushing efficiency of each crashworthiness design. The CFE is a key aspect of the load-displacement curve, reflecting the crushing characteristics of the structure. It is calculated as the ratio of the average load-to-crush force to the initial peak load (P max). The CFE values for each crashworthiness design are presented in Fig. 7c. The CT design with pure aluminum exhibits a lower CFE value of 0.44% compared to the hybrid designs, with the HICT achieving 0.50% and the HOCT reaching 0.49%. At the initial loading phase, the load-displacement curve shows a sharp drop in load after reaching the peak, followed by continued collapse at lower loads. The ratio of the average load to the peak load is sufficiently large

to indicate the composite's failure mechanism, which may be catastrophic or progressive. The slight difference in CFE values between the HICT and HOCT designs suggests that catastrophic failure occurs across all composite tubes and is influenced by the specimen's geometry [42]. In hybrid designs, high peak failure during the early crushing stage leads to an overall failure mechanism, resulting in low CFE values during the post-crush phase and unstable load-displacement behavior. However, these designs exhibit significant energy absorption when the structure fails completely [34,43].

3.4. Deformation pattern crashworthiness

The deformation pattern of crashworthiness represents the structural response to shape changes caused by impactor pressure or collision. The experimental results from quasi-static tests for each crashworthiness design are presented in Fig. 9.

Fig. 9. shows the stages of deformation during the impactor's compression of each crashworthiness design. It is evident that the deformation behavior tends to remain stable across all crashworthiness designs. Thin-walled structures, such as those used in crashworthiness applications, can exhibit three potential deformation patterns (modes) under axial loading: the concertina pattern (symmetrical mode), the diamond pattern (asymmetrical mode), and the mixed mode, which combines elements of concertina and diamond patterns [44]. The ACT design exhibits a highly stable deformation pattern throughout the crushing process, characterized by consistent folds forming a ring or concertina-like pattern (symmetrical mode). This deformation pattern demonstrates superior specific energy absorption (SEA) compared to the diamond deformation pattern typically observed in aluminum tubes. The SEA value of the ACT design is comparable to that of the HICT hybrid tube design, with only a slight difference of 0.76 kJ/kg, despite the HICT design exhibiting a diamond pattern on the metal side. Previous research has noted that ring or concertina deformation patterns generally yield higher SEA values than diamond patterns, as the concertina mode promotes greater plastic deformation and energy dissipation. [45]. This phenomenon indicates that the waru fiber composite material in hybrid tubes plays a supportive role, reinforcing the metal without compromising its structural integrity. Hybrid crashworthiness structures can exhibit six potential deformation patterns under axial loading: (1) Debris wedge formation, (2) Matrix fracture, (3) Elastic bending and pressure deformation, (4) Central delamination cracking, (5) Local buckling, and (6) Interlaminar shear or delamination [41,46].

Typical crushing modes in metal and metal-composite (hybrid) tubes are illustrated in Fig. 10. In most HICT and HOCT specimens subjected to

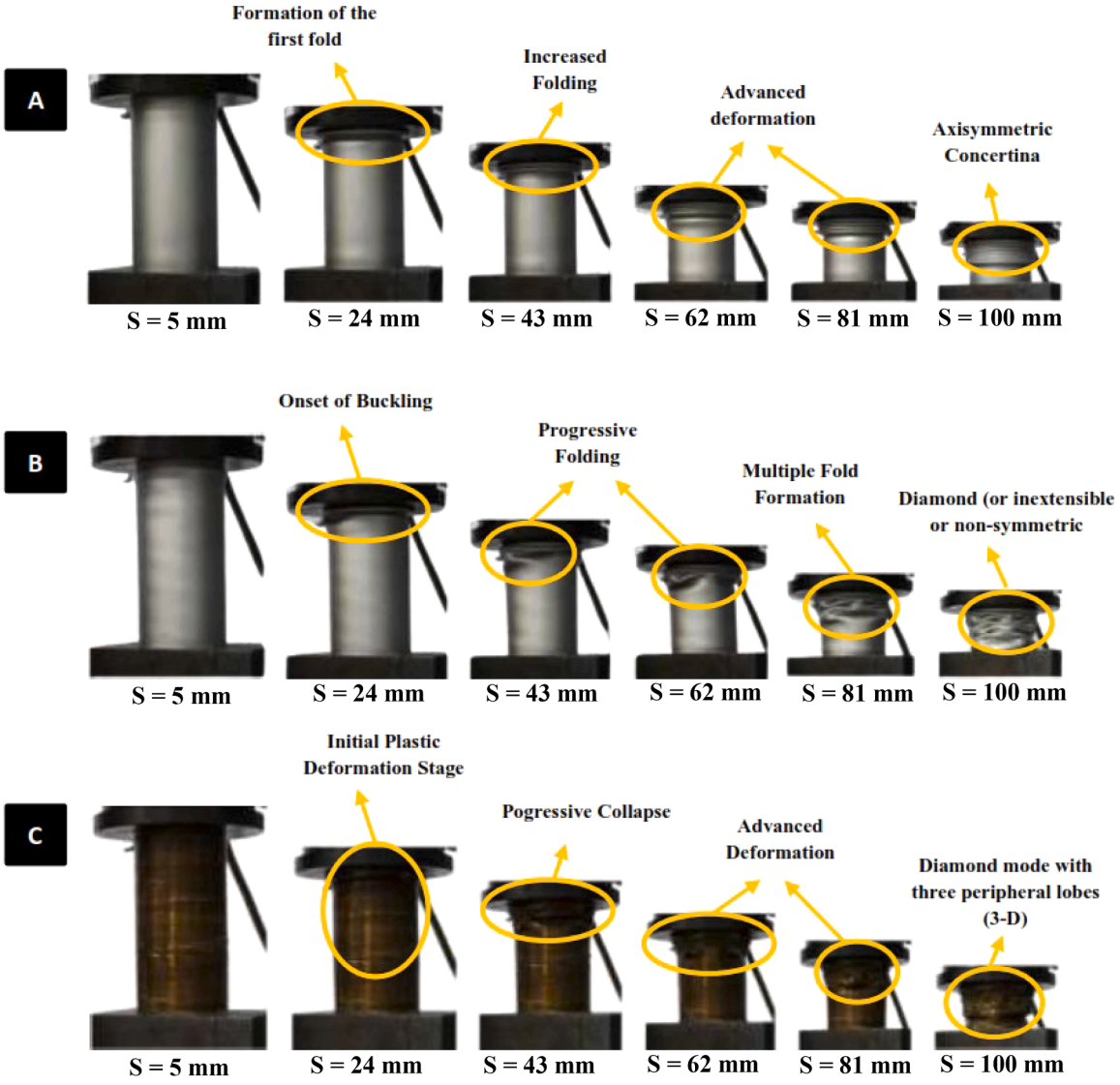

Fig. 9. Crashworthiness Deformation under Quasi-Static Loading by Time Progression (a) ACT (b) HICT (c) HOCT.

metal-fiber tube crushing, the waru fiber composite remains perfectly bonded. However, delamination is observed at the metal-composite interface, while the debonding mechanism is absent in the folds formed during the crushing process. This behavior can be attributed to the NaOH-Silane treatment applied to the waru fibers, which enhances the bonding strength between the fiber surface and the matrix, thereby improving the mechanical properties of the composite [19,18].

Most of the crushing energy is absorbed within the folds, and for average crushing loads, it can be assumed that the metal-fiber tube is perfectly bonded [47]. In the hybrid tube design, the deformation process begins with an initial force stage that counteracts the initial resistance to tube deformation; this may lead to delamination on the aluminum-composite interface. Detailed observations of the crashworthiness cross-section (Fig. 10), confirm this, supported by the high Initial Peak Force (IPFC) results. In the second stage of the load-displacement curve, the force undergoes a sharp decrease, followed by fluctuations around the average load value during the deformation process. This stage is characterized by plastic folding, elastic bending, and pressure-induced deformation. The observed fluctuations indicate the sequential progression of plastic folding.In the third stage, the force increases sharply due to reduced deformation near the end of the process, leading to the formation of curling and corkscrew deformation patterns (Fig. 11).

A detailed analysis of the crushing load ratios indicates that metal-fiber composite tubes exhibit significantly greater strength compared to their individual components. This finding underscores the critical role of the bond between the metal and composite, which consistently enhances performance regardless of the type of metal or tube geometry. Similar trends have been observed in CFRP-metal tubes [34,48]. The crushing mode of the HOCT tube demonstrates that the metal layer expands outward while compressing the external composite layer. This compression induces the composite to form additional folds (lobes), driven by the bending properties of the metal wall. The fiber composite reaches its fracture strain in regions of high curvature during lobe formation, allowing it to become trapped and facilitating the development of a corkscrew folding mechanism [49,50].

In the design of HICT tubes, the crushing mechanism involves a combination of compression and bending of the tube wall, leading to fiber strain and subsequent stress on the composite side, ultimately resulting in a curling fracture mechanism. This novel deformation pattern aligns with observations by Zhen Wang et al [51], in their study on AL-CF hybrid tubes. Their findings revealed that the deformation behavior of a single CF component in a hybrid AL-CF tube transitioned from a typical dilation mode to an internal curling mode [51]. The flexure and delamination occurring at the onset of deformation in the HICT tube caused a sudden reduction in the tube's bearing capacity, impacting its overall energy absorption efficiency.

3.5. Comparison of energy absorption CCT and ACT

Fig. 12 presents the load-displacement graph, highlighting significant differences in the mechanical properties of CCT and ACT materials. The ACT material demonstrates a higher displacement peak during the initial loading phase, indicating a lower elastic modulus and superior energy absorption capacity during the early stages of deformation. Despite its ability to sustain significant deformation under initial loading, ACT exhibits repetitive oscillatory patterns with large amplitudes that persist throughout multiple loading cycles. Conversely, the CCT material displays exceptional damping performance, characterized by an exponential reduction in amplitude that rapidly stabilizes. This behavior is attributed to the material's dominant viscoelastic properties, which allow for efficient dissipation of dynamic energy and enhanced structural stability. These features render CCT particularly suitable for applications requiring high energy dissipation efficiency and stability under dynamic loading conditions.

An analysis of the area under the load-displacement curve reveals

Fig. 10. Final deformation under quasi-static loading (a) ACT (b) HICT (c) HOCT.

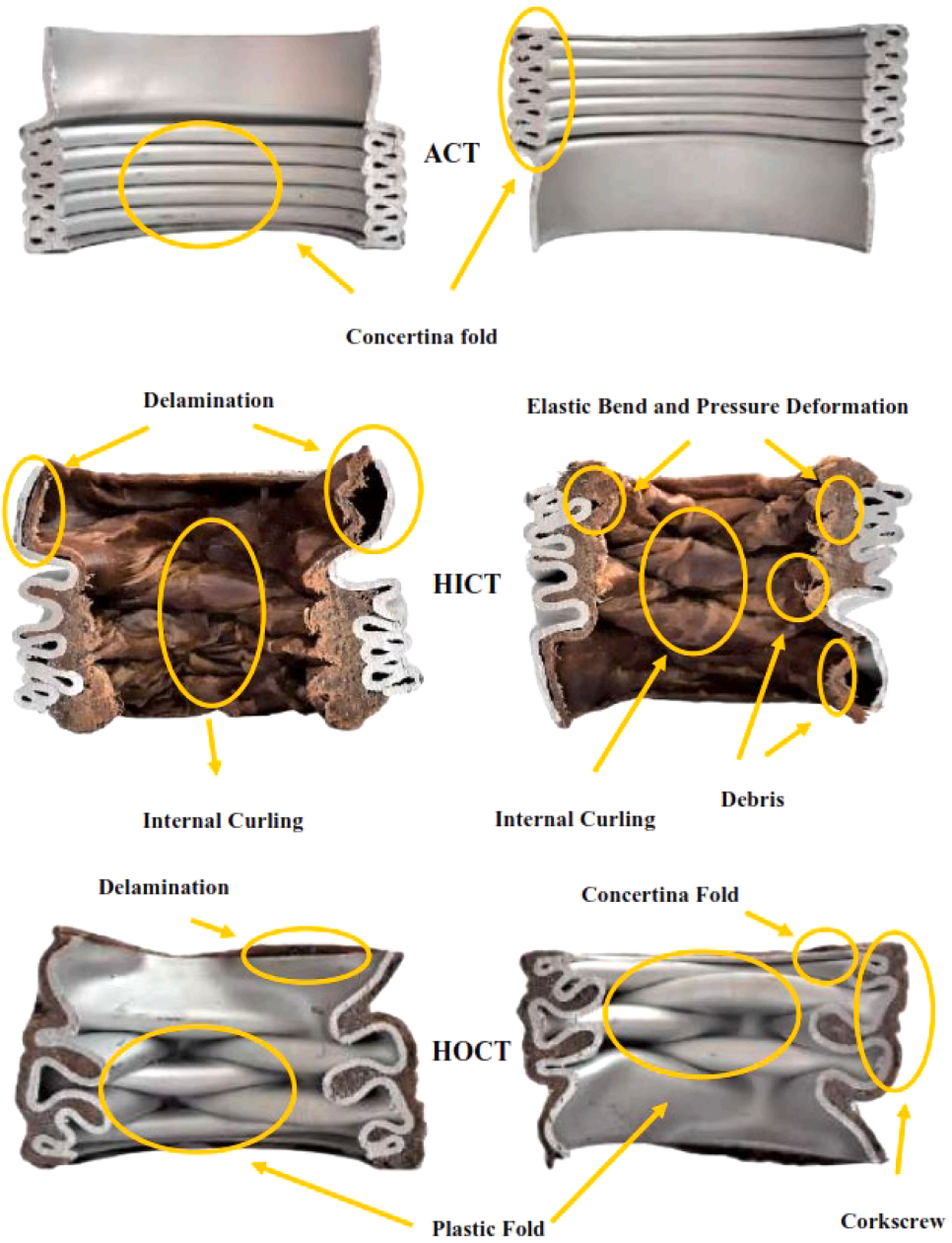

Fig. 11. Deformation Cutout of crashworthiness.

that ACT exhibits superior energy absorption capacity compared to CCT, with integrated curve values of 0.05 kJ and 0.03 kJ, respectively. This confirms the suitability of ACT for applications requiring high energy absorption, such as protective structures or impact mitigation systems. However, ACT's lower stability, as indicated by persistent displacement fluctuations, renders it less ideal for applications requiring long-term load stability, such as structural components in cyclic loading or dynamic environments. In comparison, CCT demonstrates a specific energy absorption (SEA) of 12.30 kJ/kg, Crushing Force Efficiency (CFE) of 0.268%, Initial Peak Force Capacity (IPFC) of 2.689 kN, and Maximum Force (MF) of 0.721 kJ, indicating a more balanced performance between energy absorption and structural stability. To capitalize on the strengths of both materials, a hybrid configuration combining CCT and ACT could provide an effective solution. In this arrangement, ACT would function as the energy-absorbing layer during impact events, while CCT would serve as the core layer to enhance stability and suppress excessive dynamic oscillations. This hybrid approach enables the material to achieve both high energy absorption and structural stability, making it a versatile choice for multifunctional applications [43,29,25].

Deformation in the CCT begins with local buckling under applied loading, likely attributed to the anisotropic properties of the waru composite material. The onset of local buckling results in uneven force distribution across the crashworthiness wall, leading to structural instability and the progression of global buckling (Euler buckling), which persists until the end of the test. This buckling mechanism limits the energy absorption efficiency of the waru composite tube, resulting in a relatively low energy absorption value. Hybridizing waru composite with aluminum materials significantly enhances the energy absorption capacity of the crashworthiness tube design, achieving a value of 2.76 kJ. This improvement is primarily due to the hybrid's ability to deliver a more substantial force response, attributed to increased cross-sectional inertia [37,13]. The comparison suggests that the incorporation of waru fiber composite in hybrid tubes supports the metal layer, enhancing its performance without compromising the integrity of the metal component when used independently. (Fig. 13).

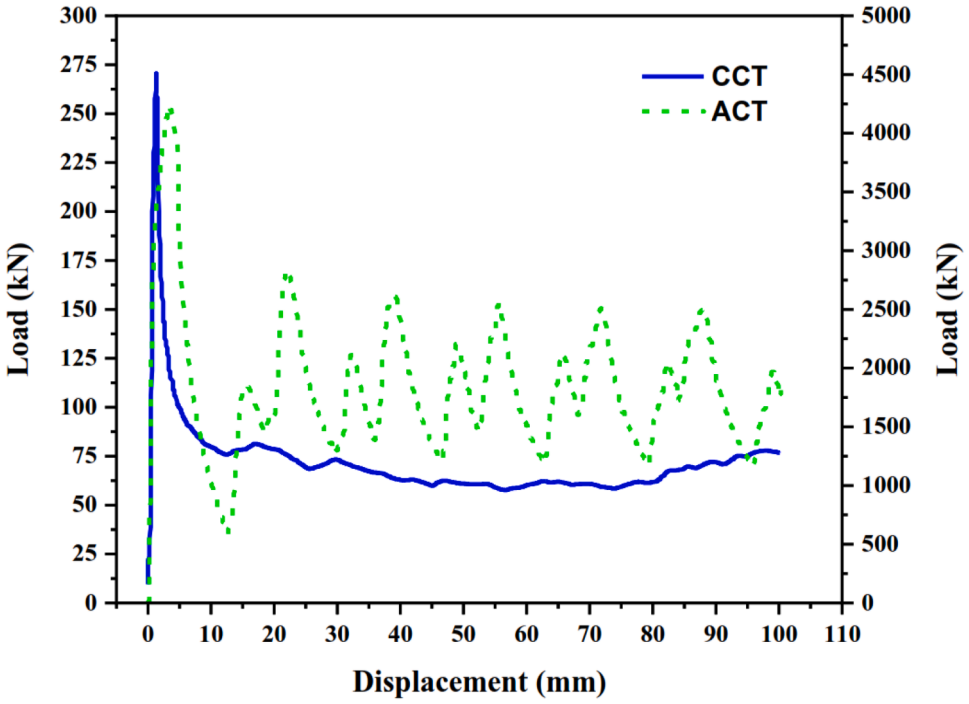

Fig. 12. Load-Displacement of CCT and ACT Materials.

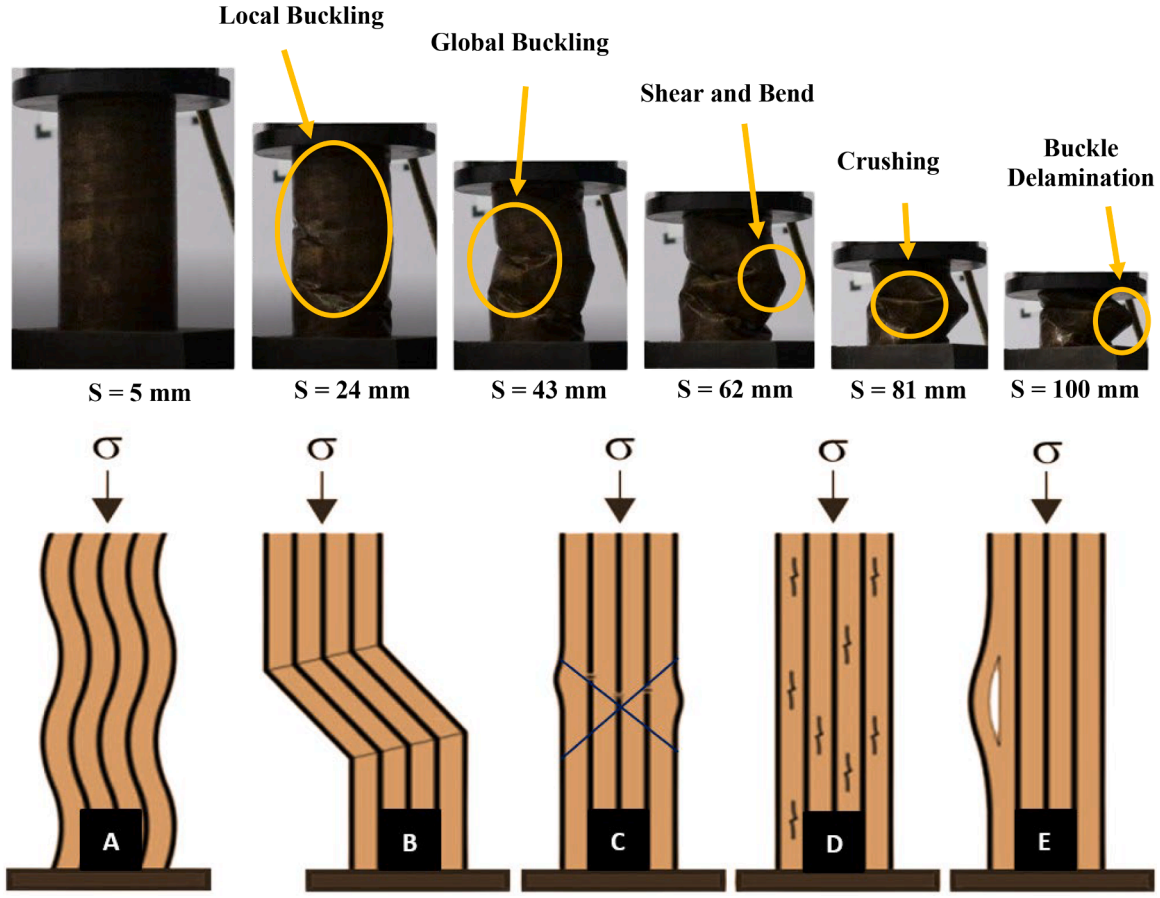

Fig. 13. Crashworthiness deformation of CCT under Quasi-static Loading based on time progression (a) Elastic micro buckling (b) Fiber Kinking (c) Fiber crushing (shear and band formation) (d) Cracking (e) Buckle delamination.

3.6. Specific energy absorption (SEA) and crushing force efficiency (CFE)

An analysis of Specific Energy Absorption (SEA) and Crushing Force Efficiency (CFE) in hybrid structures such as ACT (Aluminum Circle Tube) and CCT (Composite Circle Tube) reveals key factors in crashworthy design, ensuring safety and energy efficiency during impact. SEA measures a structure's ability to absorb energy per unit mass, which is crucial for minimizing damage during collisions. Meanwhile, CFE assesses the efficiency of impact force distribution, ensuring controlled progressive deformation without dangerous peak force spikes. A balance between both factors is essential to create designs that optimally absorb energy while maintaining force stability.

Fig. 14 represents the combination of SEA and CFE values for the CCT, ACT, HICT, and HOCT tube designs. It illustrates that an increase in Crushing Force Efficiency (CFE) does not always result in a significant improvement in Specific Energy Absorption (SEA) for each crashworthiness tube design. In the CCT design, which utilizes composite materials, the structure tends to exhibit low energy absorption, being more susceptible to damage and rapid collapse. This is further evidenced by the high Initial Peak Force (IPFC) value (stiffness) and the observed deformation patterns in CCT, which undergo several deformation mechanisms such as elastic micro-buckling, fiber kinking, fiber crushing, cracking, and buckle delamination. In contrast, the ACT configuration represents a design or material that demonstrates more elastic impact forces with a good energy absorption capacity.

The hybrid designs of HICT and HOCT tend to show higher values compared to single tubes like CCT and ACT. The combination of these two materials can lead to significant improvements in both energy absorption and force stability, as the configuration of the materials complements each other. Research across various studies indicates that increasing the thickness of aluminum tubes can enhance energy absorption (EA) and load-carrying capacity, but may reduce Crushing Force Efficiency (CFE) due to higher initial peak forces (IPFC) [29,40,52]. A combination of thin aluminum layers and more CFRP layers, such as in the hybrid tube AC-1.0-8 (1.0 mm aluminum, 8 layers of CFRP), optimizes both SEA and CFE, with better EA compared to individual materials like pure aluminum or CFRP [25].

An interesting finding in this study is that the addition of composite material on the outer surface of the HOCT tube results in a better Specific Energy Absorption (SEA) configuration compared to the addition of composite material on the inner surface of the HICT tube. Conversely, the HICT design exhibits higher Crushing Force Efficiency (CFE) than HOCT. This can be attributed to the fact that the addition of composite layers on the outer surface of the tube (as in the HOCT design) enhances the tube's ability to absorb energy (SEA), as external composite layers are more effective in dissipating and managing impact energy during the initial collapse phase. Composites possess high elasticity, which allows the HOCT tube to absorb more energy; however, the force distribution within this structure is less uniform, leading to a decrease in CFE. On the other hand, adding composite layers to the inner surface of the tube, as in the HICT design, improves the efficiency of force distribution during collapse. This helps to reduce the peak forces experienced during the initial compression phase and results in less local damage. The higher CFE observed in the HICT design indicates that it is more effective in managing compressive forces during the compression process, with a more stable force distribution and reduced potential for structural failure. The addition of composite material on the inner surface offers an advantage in terms of more uniform collapse resistance, efficiently enhancing force absorption, although its SEA is lower compared to HOCT. Overall, the differences between HOCT and HICT highlight a trade-off between SEA and CFE in hybrid composite tube design. The HOCT design emphasizes greater energy absorption, while the HICT design excels in force distribution efficiency and better management of compressive strength. Both designs can be selected based on the desired priority for crashworthiness applications, whether emphasizing energy absorption capability or efficient force distribution for optimal protection.

4. Conclusions

The experimental findings on hybrid tube design engineering demonstrate that the addition of composite reinforcement layers to aluminum significantly enhances both structural strength and energy absorption capacity. The HICT and HOCT tube designs, reinforced with

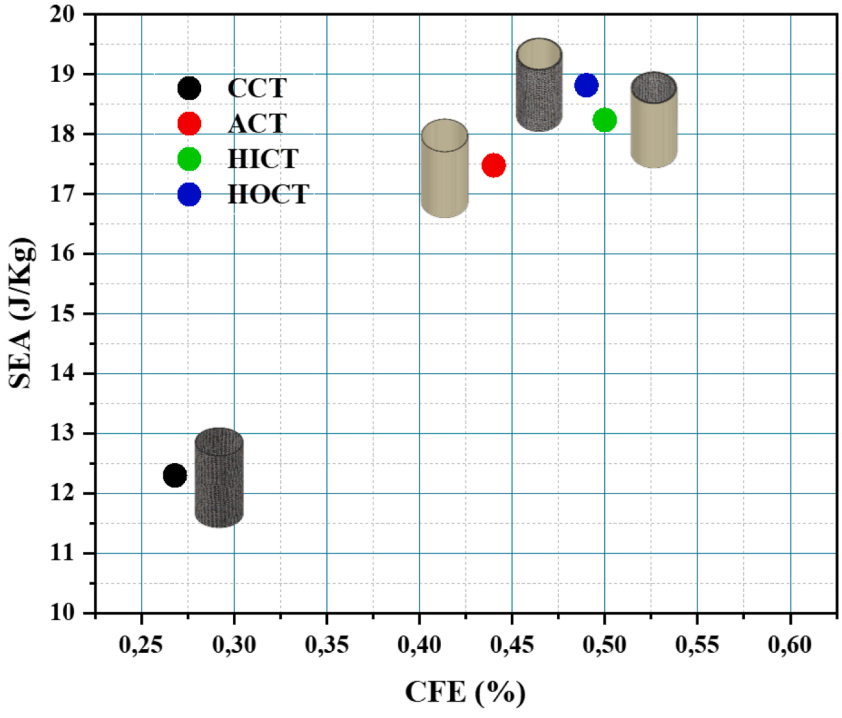

Fig. 14. SEA-CFE Configuration.

waru fiber composite layers, achieved superior energy absorption values of 2.66 kJ and 2.76 kJ, respectively, compared to the CCT and ACT tubes, which had energy absorption values of 0.05 kJ and 0.03 kJ. The HOCT tube design experienced a substantial increase in energy absorption, with a 49.18 % improvement, highlighting its potential for high-performance applications. This increase was accompanied by improvements in other performance metrics, including an IPFC value of 42.36 kN, MF of 24.66 kN, SEA value of 18.82 kN, and CFE value of 0.49 %. The deformation pattern of the HOCT tube was characterized by stability, progressive folding, and the emergence of unique curling and corkscrew mechanisms. These deformation features highlight new opportunities for developing high-performance, environmentally friendly energy-absorbing tube designs.

CRediT authorship contribution statement

Willy Artha Wirawan: Writing – review & editing, Writing – original draft, Supervision, Methodology, Investigation, Funding acquisition, Formal analysis, Data curation, Conceptualization. **Ayan Sabitah:** Resources, Project administration, Funding acquisition, Data curation. **Gunawan Sakti:** Visualization, Validation, Software, Resources, Data curation. **Bambang Bagus Harianto:** Data curation, Funding acquisition, Investigation, Writing – review & editing. **Moch. Agus Choiron:** Writing – review & editing, Validation, Supervision, Software, Methodology, Investigation. **R.A. Ilyas:** Writing – review & editing, Writing – original draft, Validation, Supervision, Conceptualization. **S.M. Sapuan:** Writing – review & editing, Validation, Supervision. **Joewono Prasetijo:** Writing – review & editing, Validation, Formal analysis, Data curation, Conceptualization.

Declaration of competing interest

The authors declare that they have no known competing financial interests or personal relationships that could have appeared to influence the work reported in this paper.

Acknowledgements

The authors would like to acknowledge the Department of Aircraft Engineering at Surabaya Aviation Polytechnic, Brawijaya University, and Universiti Putra Malaysia for their support of this work through educational and research collaborations.

Data availability

Data will be made available on request.

References

[1] M.A. Choiron, Characteristics of deformation pattern and energy absorption in honeycomb filler crash box due to frontal load and oblique load test, Eastern-Eur. J. Enterp. Technol 2 (7–104) (2020) 6–11, https://doi.org/10.15587/1729-4061.2020.200020.

[2] R. Velmurugan, R. Muralikannan, Energy absorption characteristics of annealed steel tubes of various cross sections in static and dynamic loading, Lat. Am. J. Solids Struct. 6 (4) (2009) 385–412.

[3] M.S. Ul Abrar, K.F. Nadim Ezaz, M.J. Hasan, R.I. Pranto, T.A. Alvy, M.Z. Hossain, Speed-dependent impact analysis on a car bumper structure using various materials, Results Eng. 21 (November 2023) (2024) 101927, https://doi.org/10.1016/j.rineng.2024.101927.

[4] S. Esmaeili-Marzdashti, S. Pirmohammad, S. Esmaeili-Marzdashti, Crashworthiness analysis of S-shaped structures under axial impact loading, Lat. Am. J. Solids Struct. 14 (5) (2017) 743–764, https://doi.org/10.1590/1679-78253430.

[5] J.S. Kim, H.J. Yoon, K.B. Shin, A study on crushing behaviors of composite circular tubes with different reinforcing fibers, Int. J. Impact Eng. 38 (4) (2011) 198–207, https://doi.org/10.1016/j.ijimpeng.2010.11.007.

[6] J. Marzbanrad, M.R. Ebrahimi, Multi-Objective Optimization of aluminum hollow tubes for vehicle crash energy absorption using a genetic algorithm and neural networks, Thin-Walled Struct. 49 (12) (2011) 1605–1615, https://doi.org/10.1016/j.tws.2011.08.009.

[7] S. Hou, T. Liu, Z. Zhang, X. Han, Q. Li, How does negative Poisson's ratio of foam filler affect crashworthiness? Mater. Des. 82 (2015) 247–259, https://doi.org/10.1016/j.matdes.2015.05.050.

[8] L.N.S. Chiu, et al., Crush responses of composite cylinder under quasi-static and dynamic loading, Compos. Struct. 131 (2015) 90–98, https://doi.org/10.1016/j.compstruct.2015.04.057.

[9] S. Boria, A. Scattina, G. Belingardi, Axial crushing of metal-composite hybrid tubes: Experimental analysis, Procedia Struct. Integr. 8 (2018) 102–117, https://doi.org/10.1016/j.prostr.2017.12.012.

[10] C.W. Isaac, C. Ezekwem, A review of the crashworthiness performance of energy absorbing composite structure within the context of materials, manufacturing and maintenance for sustainability, Compos. Struct. (2020) 113081, https://doi.org/10.1016/j.compstruct.2020.113081.

[11] G. Zheng, Z. Wang, K. Song, Energy absorption on metal-composite hybrid structures: Experimental and numerical simulation, Thin-Walled Struct. 150 (November 2019) (2020) 106571, https://doi.org/10.1016/j.tws.2019.106571.

[12] A. Al Ali, E. Arhore, H. Ghasemnejad, M. Yasaee, Experimental and numerical investigation of multi-layered honeycomb sandwich composites for impact mechanics applications, Results Eng. 21 (November 2023) (2024) 101817, https://doi.org/10.1016/j.rineng.2024.101817.

[13] H. Yang, H. Lei, G. Lu, Crashworthiness of circular fiber reinforced plastic tubes filled with composite skeletons/aluminum foam under drop-weight impact loading, Thin-Walled Struct. 160 (November 2020) (2021) 107380, https://doi.org/10.1016/j.tws.2020.107380.

[14] X. Han, Z. Zhang, Y. Pan, G.C. Barber, H. Yang, F. Qiu, Sliding wear behavior of laser surface hardened austempered ductile iron, J. Mater. Res. Technol. 9 (6) (2020) 14609–14618, https://doi.org/10.1016/j.jmrt.2020.10.050.

[15] J. Ke, L. Liu, Z. Wu, Z. Le, L. Bao, D. Luo, Torsional mechanical properties and damage mechanism of glass fiber-ramie hybrid circular tube, Compos. Struct. 327 (August 2023) (2024) 117680, https://doi.org/10.1016/j.compstruct.2023.117680.

[16] N.F. Apriliani, W.A. Wirawan, M. Muslimin, R.A. Ilyas, M.A. Rahma, A.T.A. Salim, Improving wear performance, physical, and mechanical properties of iron sand/epoxy composite modified with carbon powder, Results Mater. 21 (73) (2024) 100532, https://doi.org/10.1016/j.rinma.2024.100532.

[17] H.M. Akil, M.F. Omar, A.A.M. Mazuki, S. Safiee, Z.A.M. Ishak, A.A. Bakar, Kenaf fiber reinforced composites : A review, Mater. Des. 32 (8–9) (2011) 4107–4121, https://doi.org/10.1016/j.matdes.2011.04.008.

[18] W.A. Wirawan, M.A. Choiron, E. Siswanto, T.D. Widodo, Analysis of the fracture area of tensile test for natural woven fiber composites (hibiscus tiliaceus-polyester), J. Phys. Conf. Ser. 1700 (1) (2020), https://doi.org/10.1088/1742-6596/1700/1/012034.

[19] W.A. Wirawan, M.A. Choiron, E. Siswanto, T.D. Widodo, Morphology, structure, and mechanical properties of new natural cellulose fiber reinforcement from waru (Hibiscus Tiliaceus) bark, J. Nat. Fibers (2022), https://doi.org/10.1080/15440478.2022.2060402.

[20] A.B.M. Supian, S.M. Sapuan, M.Y.M. Zuhri, E.S. Zainudin, H.H. Ya, H.N. Hisham, Effect of winding orientation on energy absorption and failure modes of filament wound kenaf /glass fibre reinforced epoxy hybrid composite tubes under intermediate-velocity impact (IVI) load, J. Mater. Res. Technol. 0 (2020) 1–14, https://doi.org/10.1016/j.jmrt.2020.11.103.

[21] M.F.M. Alkbir, S.M. Sapuan, A.A. Nuraini, M.R. Ishak, Fibre properties and crashworthiness parameters of natural fibre-reinforced composite structure: a literature review, Compos. Struct. 148 (2016) 59–73, https://doi.org/10.1016/j.compstruct.2016.01.098.

[22] A.B.M. Supian, S.M. Sapuan, M.Y.M. Zuhri, E.S. Zainudin, H.H. Ya, Hybrid reinforced thermoset polymer composite in energy absorption tube application: a review, Def. Technol. 14 (4) (2018) 291–305, https://doi.org/10.1016/j.dt.2018.04.004.

[23] A.B.M. Supian, S.M. Sapuan, M.Y.M. Zuhri, E.S. Zainudin, H.H. Ya, Crashworthiness performance of hybrid kenaf/glass fiber reinforced epoxy tube on winding orientation effect under quasi-static compression load, Def. Technol. 16 (5) (2020) 1051–1061, https://doi.org/10.1016/j.dt.2019.11.012.

[24] Z. Zhang, S. Hou, Q. Liu, X. Han, Winding orientation optimization design of composite tubes based on quasi-static and dynamic experiments, Thin-Walled Struct. 127 (November 2017) (2018) 425–433, https://doi.org/10.1016/j.tws.2017.11.052.

[25] Z. Zhang, Q. Liu, J. Fu, Y. Lu, Thin-Walled Structures Parametric study on the crashworthiness of the Al /CFRP / GFRP hybrid tubes under quasi-static crushing, Thin Walled Struct. 192 (August) (2023), https://doi.org/10.1016/j.tws.2023.111156.

[26] M. Azeem, et al., Impact response of filament-wound structure with polymeric liner: Experimental and numerical investigation (Part-A), Results Eng. 21 (December 2023) (2024) 101730, https://doi.org/10.1016/j.rineng.2023.101730.

[27] R.A. Eshkoor, S.A. Oshkovr, A.B. Sulong, R. Zulkifli, A.K. Ariffin, C.H. Azhari, Effect of trigger configuration on the crashworthiness characteristics of natural silk epoxy composite tubes, Compos. Part B 55 (1) (2013) 5–10, https://doi.org/10.1016/j.compositesb.2013.05.022.

[28] S.N. Fitriah, M.S. Abdul Majid, M.J.M. Ridzuan, R. Daud, A.G. Gibson, T. A. Assaleh, Influence of hydrothermal ageing on the compressive behaviour of glass fibre/epoxy composite pipes, Compos. Struct. 159 (2017) 350–360, https://doi.org/10.1016/j.compstruct.2016.09.078.

[29] S. Li, On lateral crashworthiness of aluminum /composite hybrid structures, Compos. Struct. 245 (February) (2020) 112334, https://doi.org/10.1016/j.compstruct.2020.112334.

[30] W.A. Wirawan, Surface modification with silane coupling agent on tensile properties of natural fiber composite, J. Energy Mech. Mater. Manuf. Eng. 2 (2) (2017) 98–105, https://doi.org/10.22219/jemmme.v2i2.5053.
[31] W.A. Wirawan, et al., Collapse behavior and energy absorption characteristics of design multi-cell thin wall structure 3D-printed under quasi statistic loads, Automot. Exp. 7 (1) (2024) 149–160, https://doi.org/10.31603/ae.10892.
[32] C. William, C. Ezekwem, A review of the crashworthiness performance of energy absorbing composite structure within the context of materials, manufacturing and maintenance for sustainability, Compos. Struct. 257 (August 2020) (2021) 113081, https://doi.org/10.1016/j.compstruct.2020.113081.
[33] W. Abramowicz, The effective crushing distance in axially compressed thin-walled metal columns, Int. J. Impact Eng. 1 (3) (1983) 309–317, https://doi.org/10.1016/0734-743X(83)90025-8.
[34] M.R. Bambach, Axial capacity and crushing of thin-walled metal, fibre-epoxy and composite metal-fibre tubes, Thin-Walled Struct. 48 (6) (2010) 440–452, https://doi.org/10.1016/j.tws.2010.01.006.
[35] S. Gowid, E. Mahdi, J. Renno, S. Sassi, G. Kharmanda, A. Shokry, Experimental investigation of the crashworthiness performance of fiber and fiber steel-reinforced composites tubes, Compos. Struct. 251 (2020), https://doi.org/10.1016/j.compstruct.2020.112655.
[36] H. Yang, H. Lei, G. Lu, Z. Zhang, X. Li, Y. Liu, Energy absorption and failure pattern of hybrid composite tubes under quasi-static axial compression, Compos. Part B 198 (July) (2020) 108217, https://doi.org/10.1016/j.compositesb.2020.108217.
[37] M. Mirzaei, M. Shakeri, M. Sadighi, H. Akbarshahi, Experimental and analytical assessment of axial crushing of circular hybrid tubes under quasi-static load, Compos. Struct. 94 (6) (2012) 1959–1966, https://doi.org/10.1016/j.compstruct.2012.01.003.
[38] G. Zhu, G. Sun, H. Yu, S. Li, Q. Li, Energy absorption of metal, composite and metal/composite hybrid structures under oblique crushing loading, Int. J. Mech. Sci. 135 (November 2017) (2018) 458–483, https://doi.org/10.1016/j.ijmecsci.2017.11.017.
[39] M. Harhash, M. Kuhtz, J. Richter, A. Hornig, M. Gude, H. Palkowski, Trigger geometry influencing the failure modes in steel/polymer/steel sandwich crashboxes: Experimental and numerical evaluation, Compos. Struct. 262 (January) (2021) 113619, https://doi.org/10.1016/j.compstruct.2021.113619.
[40] H. Yang, Y. Ren, Crashworthiness design of CFRP /AL hybrid circular tube under lateral crushing, Thin-Walled Struct. 186 (February) (2023) 110669, https://doi.org/10.1016/j.tws.2023.110669.
[41] C. Reuter, T. Tröster, Crashworthiness and numerical simulation of hybrid aluminium-CFRP tubes under axial impact, Thin-Walled Struct. 117 (September 2016) (2017) 1–9, https://doi.org/10.1016/j.tws.2017.03.034.
[42] S.A. Oshkovr, R.A. Eshkoor, S.T. Taher, A.K. Ariffin, C.H. Azhari, Crashworthiness characteristics investigation of silk /epoxy composite square tubes Crashworthiness characteristics investigation of silk / epoxy composite square tubes, Compos. Struct. 94 (8) (2012) 2337–2342, https://doi.org/10.1016/j.compstruct.2012.03.031.
[43] A.P. Kumar, D. Maneiah, L.P. Sankar, Improving the energy-absorbing properties of hybrid aluminum-composite tubes using nanofillers for crashworthiness applications, *Proc. Inst. Mech. Eng. Part C* 0 (0) (2020) 1–12, https://doi.org/10.1177/0954406220942267.
[44] H. Halman, M. Choiron, D. Darmadi, Pengaruh variasi sambungan pada crash box multi segmen terhadap kemampuan penyerapan energi dengan Uji Quasi Static, J. Rekayasa Mesin 9 (1) (2018) 43–49, https://doi.org/10.21776/ub.jrm.2018.009.01.7.
[45] K.R.F. Andrews, G.L. England, E. Ghani, Classification of the axial collapse of cylindrical tubes under quasi-static loading, Int. J. Mech. Sci. 25 (9–10) (1983) 687–696, https://doi.org/10.1016/0020-7403(83)90076-0.
[46] G. Zhu, G. Sun, Q. Liu, G. Li, Q. Li, On crushing characteristics of different configurations of metal-composites hybrid tubes, Compos. Struct. 175 (2017) 58–69, https://doi.org/10.1016/j.compstruct.2017.04.072.
[47] M.R. Bambach, H.H. Jama, M. Elchalakani, Axial capacity and design of thin-walled steel SHS strengthened with CFRP, Thin-Walled Struct. 47 (10) (2009) 1112–1121, https://doi.org/10.1016/j.tws.2008.10.006.
[48] S. Ming, et al., The crashworthiness design of metal /CFRP hybrid tubes based on origami-ending approach : experimental research, Compos. Struct. 279 (June 2021) (2022) 114843, https://doi.org/10.1016/j.compstruct.2021.114843.
[49] M.R. Bambach, M. Elchalakani, Plastic mechanism analysis of steel SHS strengthened with CFRP under large axial deformation, Thin-Walled Struct. 45 (2) (2007) 159–170, https://doi.org/10.1016/j.tws.2007.02.004.
[50] R. Jiang, et al., Energy absorption characteristics of a cfrp-al hybrid thin-walled circular tube under axial crushing, Aerospace 8 (10) (2021), https://doi.org/10.3390/aerospace8100279.
[51] Z. Wang, X. Jin, Q. Li, G. Sun, On crashworthiness design of hybrid metal-composite structures, Int. J. Mech. Sci. 171 (September 2019) (2020) 105380, https://doi.org/10.1016/j.ijmecsci.2019.105380.
[52] G. Zhu, Z. Zhao, Z. Wang, L. Wei, X. Zhao, Crashworthiness analysis and design optimization of square aluminum/CFRP hybrid structures under quasi-static axial loading, Struct. Multidiscip. Optim. 67 (3) (2024) 1–24, https://doi.org/10.1007/s00158-024-03743-9.